

Intraoperative angiography of the neurovascular bundle using indocyanine green and near-infrared fluorescence improves anatomical dissection during robot-assisted radical prostatectomy: initial clinical experience

Nordine Amara (✉ nordineamara@gmail.com)

Centre Hospitalier Dunkerque

Tarek Al Youssef

Centre Hospitalier Dunkerque

Jordan Massa

Centre Hospitalier Dunkerque

Aouad Fidjel

Centre Hospitalier Dunkerque

Elias El Khoury

Centre Hospitalier Dunkerque

Belur Patel

Baylor Scott & White Hospital

Mathias Flais

Centre Hospitalier Dunkerque

Christophe Deswarte

Centre Hospitalier Dunkerque

Research Article

Keywords: Angiography, Erectile dysfunction, Indocyanine green, Near-infrared fluorescence, Robot-assisted radical prostatectomy

Posted Date: April 12th, 2022

DOI: <https://doi.org/10.21203/rs.3.rs-1538409/v1>

License: © ⓘ This work is licensed under a Creative Commons Attribution 4.0 International License.

[Read Full License](#)

Abstract

Background: Landmark artery identification in the neurovascular bundle (NVB) is important for nerve-sparing in radical prostatectomy. We aimed to investigate intraoperative angiography using indocyanine green and near-infrared fluorescence (ICG-NIRF) during robot-assisted radical prostatectomy (RARP) to identify the NVB, visualise vascularisation and haemostasis, and preserve erectile function.

Methods: Retrospective, unicentric study of 91 consecutive localised prostate cancer RARP patients (stage T1/T2, prostate specific antigen <10 ng/ml) who underwent ICG-NIRF angiography in France (2016–2021). When ready to dissect the NVB, the anaesthesiologist intravenously injected ICG (3 ml); the surgeon used alternating standard light or fluorescence to optimise NVB visualisation and facilitate microdissection. Primary outcomes: safety and feasibility of ICG-NIRF. Secondary outcomes: functional erectile dysfunction (Sexual Health Inventory for Men questionnaire) over 9 months, proportion of bilateral NVBs identified, ICG-related complications. Standard descriptive statistics were used; t-test determined the significance of changes in SHIM scores versus baseline.

Results: Ninety-one patients received intraoperative angiography. The NVB was identified in all cases, without difficulties. No ICG-related complications or allergies were observed. There was no significant difference in the SHIM score at 9 months compared with baseline ($p=0.331$), and erectile dysfunction returned to baseline levels in almost all patients.

Conclusions: Intraoperative, real-time ICG-NIRF angiography is simple, non-invasive, and improves identification of key anatomical landmarks to optimise micropreservation of the NVB during RARP and preserve erectile function. Larger clinical studies should confirm preliminary results.

Introduction

Advances in surgical techniques, combined with a greater knowledge of prostate anatomy, have enabled improved cancer control and functional outcomes [1]. During radical prostatectomy, lack of identification of anatomical landmarks may potentially have an adverse impact on oncologic results and result in a higher risk of erectile dysfunction (ED). For example, identification of the artery in the neurovascular bundle (NVB) is important for nerve-sparing [1].

To enhance real-time visualisation of structures during surgery, the new technique of optical imaging using near-infrared (700–900 nm) fluorescence (NIRF) was developed. Advantages of NIRF include high tissue penetration (depth of millimetres to centimetres) and low autofluorescence, thereby providing a good contrast [2]. The da Vinci Xi® Surgical System (Intuitive Surgical, Sunnydale, CA, USA) has a built-in NIRF visualisation system (Firefly®, Novadaq Technologies, Mississauga, ON, Canada) that can detect indocyanine green (ICG) dye in real-time. This fluorescent molecule binds rapidly and almost completely to serum proteins [3] and is carried by albumin in blood. Protein binding reduces aggregation, increases brightness (i.e. quantum yield) by over threefold, and increases the effective hydrodynamic diameter to that of the bound proteins [4, 5]. ICG is associated with favourable characteristics such as confinement to

the vascular compartment by binding to plasma proteins, fast and almost exclusive excretion into the bile, and very low toxicity [4, 6]. Intravenously-delivered ICG may be used to identify vessel perfusion and differentiate tissue density [7, 8]. In plasma, ICG has an absorption peak around 807 nm and an emission peak around 822 nm, which is within the NIRF window. Incident infrared (IR) light at a wavelength of 780 nm provokes detectable photon emission at 820–830 nm [4]. The IR laser from the illuminator causes the ICG to fluoresce, which is picked up by the endoscope signal detector (IR camera) and relayed to the console, where the surgeon visualises vessels containing the albumin-bound ICG as green, fluorescent structures. After intravenous administration, ICG has a short blood half-life (150–180 s) and is cleared exclusively by the liver [9]. The safety profile of ICG is favourable when used at the standard dose for diagnostic procedures (between 0.1 and 0.5 mg/kg). Above 0.5 mg/kg, the incidence of immediate allergic reactions increases [10]. The adverse event rate reported with ICG is 0.34%, including nausea, vomiting, and rarely shock (1 in 300,000 patients) [11].

The use of ICG with an NIRF imaging system (Akorn, Lake Forest, IL) has been described as an adjunct during robot-assisted partial nephrectomy, to help identify the renal artery and parenchymal perfusion [12]; this has become a consolidated technology to visualise edge lesions in laparoscopic, robot-assisted, nephron-sparing surgery [13]. Moreover, ICG-NIRF is used for endoscopic marking of colorectal tumours and intraoperative identification of certain solid tumours after intravenous injection [14, 15]. It may also be used during prostatectomy to visualise sentinel prostatic drainage because of the ability of ICG to mark the target prostate tissue with limited diffusion, acting as a lymphangiography agent [16].

We aimed to assess the value of ICG-NIRF in identifying the NVB, visualising vascularisation and haemostasis, and improving the preservation of ED in laparoscopic robot-assisted radical prostatectomy (RARP). Our primary outcome was the safety and feasibility of ICG-NIRF, while secondary outcomes included functional erectile dysfunction over 9 months, the proportion of bilateral NVBs identified, and ICG-related complications.

Patients And Methods

Between June 2016 and February 2021, patients with localised prostate cancer at the Urology Oncology department of the Centre Hospitalier Dunkerque, France, were treated by RARP (da Vinci Xi). In patients who met the inclusion criteria (stage T1 and T2 (stage T3 excluded), mild-moderate ED (assessed using the Sexual Health Inventory for Men scores or SHIM Score), prostate specific antigen < 10 ng/ml), we used intraoperative ICG-NIRF angiography (using the built-in Firefly fluorescence imaging system). All patients provided signed informed consent for inclusion in our study.

Operative details

The procedure was performed via a laparoscopic robotic approach, using the same technique in each patient. We dissect the seminal vesicles (SV) using a posterior approach (although this can be done anteriorly after dropping the bladder). All procedures are performed under general anaesthesia. The

patient is positioned securely on the operating table with stirrups, then prepped and draped. After completion of the standard “time-out”, a Foley catheter is inserted. Next, a Veress needle is placed in Palmer's point in the left upper quadrant. Once the needle reaches the peritoneal cavity, carbon dioxide is pumped into the abdomen via tubing from an insufflator, creating a pneumoperitoneum. As the pressure slowly rises, the port sites are prepared. The first port (the camera port) is placed through a transverse incision just above the navel followed by the remaining five ports, all under direct vision. Once all ports are ready, the patient is placed in the Trendelenburg position, allowing gravity to gently pull the abdominal contents out of the pelvis, facilitating access to the bladder and prostate and reducing the risk of injury to abdominal organs. Once the patient is positioned, the robot is docked (side docking is usually performed).

Angiography protocol

All included patients underwent the same angiography protocol. When the NVB is ready to dissect, the anaesthesiologist intravenously injects ICG (3 ml). In our experience, the key to mobilisation of the SV is to focus on lifting them with minimal traction to the surrounding hypogastric nerve. ICG helps us to control this traction under direct visualisation of the vessels in the NVB (good traction means that the NVB is still « bleeding green slowly »). The SV are then used to lift the prostate for separation from the rectum. The denonvilliers fascia is grasped and lifted and incised sharply until the perirectal fat is seen. Dissection of the plane between the prostate and rectum is facilitated by the surgeon's left hand elevating the prostate as the assistant gently but firmly retracts the rectum with the sucker as needed.

Microdissection is performed using non-electrified scissors and the Hem-o-lok Ligation System (Teleflex, USA). Intraoperative, real-time angiography using alternating fluorescent and standard light (Fig. 1) helps us to accurately visualise the NVB, carry out microdissection (Fig. 2), and facilitate preservation. The dissection is carried distally to the apex. This approach to the nerve bundles of the prostatic pedicles focuses on minimising traction. Holding the prostate with the fourth arm and sharply releasing the nerve from the prostate without traction is critical to nerve preservation. See the Supplementary Video for further details on the standard technique for angiographic surgery of the NVB performed in our Urology unit.

Outcomes assessed

We evaluated the proportion (%) of bilateral NVB identified to optimise and facilitate the dissection, as well as any ICG-related complications that occurred (assessed using the Clavien-Dindo classification [17]). All patients were followed up at 3, 6, 9, and 12 months after surgery to evaluate their erectile function using the SHIM score.

Statistical analysis

Continuous variables are presented as mean \pm standard deviation (median; minimum–maximum or quartiles Q1-Q3) while categorical variables are presented by frequency and percentage. The significance of the change in SHIM score at 3, 6 and 9 months compared to baseline was determined using the t-test.

To evaluate the impact of BMI on results, correlations were assessed between BMI, SHIM scores at each time point, and changes in SHIM scores at each time point using both Pearson's (linear correlation) and Spearman's (non-parametric method able to detect correlations of any forms) coefficients. The significance of association between being obese and SHIM (scores + changes in scores) was also calculated using the t-test. The significance of association between obesity and being in a moderate or severe ED category was determined using the Chi-square or exact Fisher's test (depending on the sample size in each category). Statistical analyses were done with Stata version 14.2.

Results

Patient characteristics

Between June 2016 and February 2021, 207 patients with localised prostate cancer were treated by RARP in our Urology unit. We used ICG-NIRF angiography in 91 patients who met the inclusion criteria (mean age 67.8 ± 5.9 years) (Table 1). Of these, 45 patients (49.5%) were obese (BMI ≥ 30). Before surgery, the mean PSA level was 6.7 ± 1.8 ng/ml. Most patients were stage T2c (48 patients, 52.8%) and had a Gleason score of 6 (53 patients, 58.2%).

Operative details

The mean operating time was 104.3 ± 32.1 (90; min.-max. 68–223) min. Mean blood loss was 271.3 ± 128.5 (234; min.-max. 9-800) ml. Using NIRF, the prostatic arterial structure was visualised 30-60 seconds after injection of the ICG and we were able to optimally highlight the bilateral NVB in all patients (100%), without any difficulties. The procedure was simple, allowing us to easily dissect the lateral pedicles and control arterial flow and haemostasis. We were able to perform the dissection using an alternating NIRF and non-IR view in each patient (Figs. 1 & 2). There was no increase in operative times for this procedure compared with RARP without ICG injection. No complications related to the ICG injection were reported.

Erectile dysfunction

At baseline, the average SHIM score was 16.7 and all patients had some signs of ED, mostly mild (67.0%) or mild-to-moderate (26.4%) (Table 1). After surgery, there was a significant decrease (i.e., deterioration) in the SHIM score at 3 and 6 months ($p < 0.001$ and $p = 0.008$, respectively; Table 2). The proportion of patients with mild or mild-to-moderate ED also decreased at 3 months (44.0% and 37.4%, respectively) and 6 months (52.8% and 31.9%) (Fig. 3). However, at 9 months there was no significant difference in the SHIM score compared with baseline ($p = 0.331$), and most patients once again reported mild (65.9%) or mild-to-moderate (25.3%) ED. Overall, ED remained stable or showed improvement in 49.5% of patients at 3 months, 57.1% at 6 months, and 75.8% at 9 months (Table 3).

Impact of BMI on ED. We found no significant correlation between BMI and ED, or between obesity ($\text{BMI} \geq 30$) and the SHIM score (Supplementary Table 1). It was noted, however, that a greater proportion of patients with moderate or severe ED were in the obese category at baseline and throughout follow-up.

Sensitivity analysis. Two patients were excluded from the longitudinal assessment of SHIM due to the occurrence of other events impacting on these results (patient 60 had a cardiac infection 16 weeks after surgery; patient 72 was diagnosed with leukaemia 3 months after surgery). Exclusion of these patients in the sensitivity analysis did not significantly alter the impact on ED, apart from a significantly higher SHIM score (17.3 ± 2.5 vs. 15.6 ± 4.4 ; $p=0.032$) and change from baseline (0.04 ± 1.1 vs. -0.5 ± 1.4 ; $p=0.035$) at 9 months in non-obese vs. obese patients, respectively.

Discussion

The introduction of anatomical nerve-sparing techniques has been one of the most significant advances in urology and the surgical management of prostate cancer [1]. Patients expect to be potent after surgery, and these procedures have helped to improve radical prostatectomy in cases where impotence was occurring [18].

Near-infrared fluorescent imaging with ICG is an emerging technology that is gaining acceptance for being a valid tool in the decision making of surgeons. ICG binds to plasma lipoproteins if injected intravenously and, when excited by NIRF, provides anatomic information about the vascularisation of organs and tissue perfusion. ICG-NIRF is a simple, fast, and reproducible method capable of intraoperatively visualising and assessing the NVB and optimising dissection. Authorisation of ICG by the FDA and European Medicines Agency means that it has been the subject of a large number of studies. However, reliable scoring/grading parameters related to the ICG signal need to be defined. Additionally, more prospective, randomised, and adequately powered studies are required to reveal the true potential of this surgical technological innovation.

Kumar et al. highlighted the importance of the prostatic landmark artery (LA) in nerve-sparing RARP [19]. However, identification of the LA might be difficult for a novice surgeon and in patients with adverse anatomy. Use of ICG-NIRF technology during RARP has the potential to enable accurate identification of the LA and its pathway, which could help both experienced and novice surgeons in NVB preservation and improve the quality of nerve sparing [1]. In our study, ICG (3 ml) was injected intravenously in 91 patients undergoing nerve-sparing RARP. The optimal time for the ICG injection was a big challenge, but we determined it to be after incision of the bladder neck and dissection of seminal vesicles. Only after visualising the location of the arteries using NIRF technology (30–60 seconds after ICG injection) did we proceed to resect the bilateral pedicles. In all patients, the console operator was able to view the location and pathway of the artery as a green, fluorescent vessel over the lateral surface of the prostate, allowing easy dissection of the lateral pedicles and good control of arterial flow and haemostasis. The use of ICG did not increase the operating time or the risk of immediate or long-term complications.

Our findings are comparable to those reported in other studies. Kumar et al. examined the effectiveness of NIRF and ICG technology in identifying the prostatic artery in the first ten prospective cases of nerve-sparing RARP [19]. This technology helped when revising the plane of NVB dissection, and allowed identification of the LA and its pathway in 85% cases. Mangano et al. identified the prostatic arteries and NVB using NIRF technology in all of their patients [20], albeit in a limited number of patients (n = 26). Similarly, we were able to visualise the NVB in all 91 patients in our study.

The limited number of patients included in our study may affect generalisation of the results, combined with the fact that the majority had mild or mild-to-moderate ED at baseline. However, it is important to note the importance of the concept of regaining erectile function to a level that is back to baseline [21]. We found that erectile function had returned to baseline levels in most patients at 9 months (Fig. 3).

Conclusions

Fluorescence-guided surgery is a simple, promising, and non-invasive technique that can help reveal and identify key anatomical landmarks to optimise NVB micropreservation and potentially preserve erectile function. In our experience in a limited number of patients, use of ICG-NIRF during RARP helped to facilitate identification of the prostatic landmark artery of the NVB. The technique makes the procedure easier for the urologist, could be useful in preserving the NVB and erectile function without causing any complications, and represents a new way for anatomical experts to study and visualise the NVB and surrounding complex anatomy.

Declarations

Acknowledgements

Statistical analysis was performed by Corinne Le Reun (Freelance Senior Biostatistician, St Anne, Guadeloupe). The manuscript was drafted by a medical writer, Deborah Nock (Medical WriteAway, Norwich, UK).

Funding

The services of the medical writer (a native English speaker) were funded by Intuitive Surgical Sàrl. Otherwise, the authors declare no funding for this study.

Competing interests

The authors declare that there are no competing interests.

Author contributions

Conception and design: Nordine Amara; Acquisition of data: all authors; Analysis and interpretation of data: Nordine Amara (Corinne Le Reun); Drafting of the manuscript: Nordine Amara; Critical revision of

the manuscript for important intellectual content: Nordine Amara, Belur Patel, Elias El Khoury, Tarek Al Youssef; Statistical analysis: Nordine Amara (Corinne Le Reun); Obtaining funding: Nordine Amara (for medical writer); Administrative, technical or material support: Nordine Amara; Supervision: all authors.

Ethics approval

No ethical approval was required because the molecule is widely used with no side effects.

Informed consent

Informed consent was obtained from all individual participants included in the study.

Consent to publish

Not applicable.

References

1. Walz J, Epstein JI, Ganzer R, Graefen M, Guazzoni G, Kaouk J, et al. (2016). A Critical Analysis of the Current Knowledge of Surgical Anatomy of the Prostate Related to Optimisation of Cancer Control and Preservation of Continence and Erection in Candidates for Radical Prostatectomy: An Update. *Eur Urol* 70:301–311. doi: 10.1016/j.eururo.2016.01.026.
2. Frangioni JV (2008). New technologies for human cancer imaging. *J Clin Oncol* 26:4012–4021. doi: 10.1200/JCO.2007.14.3065.
3. Egloff-Juras C, Bezdetnaya L, Dolivet G, Lassalle HP (2019). NIR fluorescence-guided tumor surgery: new strategies for the use of indocyanine green. *Int J Nanomedicine* 14:7823–7838. doi: 10.2147/ijn.S207486.
4. Landsman ML, Kwant G, Mook GA, Zijlstra WG (1976). Light-absorbing properties, stability, and spectral stabilization of indocyanine green. *J Appl Physiol* 40:575–583. doi: 10.1152/jappl.1976.40.4.575.
5. Ohnishi S, Lomnes SJ, Laurence RG, Gogbashian A, Mariani G, Frangioni JV (2005). Organic alternatives to quantum dots for intraoperative near-infrared fluorescent sentinel lymph node mapping. *Mol Imaging* 4:172–181. doi: 10.1162/15353500200505127.
6. Alford R, Simpson HM, Duberman J, Hill GC, Ogawa M, Regino C, et al. (2009). Toxicity of organic fluorophores used in molecular imaging: literature review. *Mol Imaging* 8:341–354. doi: 10.2310/7290.2009.00031.
7. Choi M, Choi K, Ryu S-W, Lee J, Choi C (2011). Dynamic fluorescence imaging for multiparametric measurement of tumor vasculature. *J Biomed Opt* 16:046008–046008. doi: 10.1117/1.3562956.
8. Schaafsma BE, Mieog JSD, Hutteman M, van der Vorst JR, Kuppen PJK, Löwik C, W. G. M., et al. (2011). The clinical use of indocyanine green as a near-infrared fluorescent contrast agent for image-guided oncologic surgery. *J Surg Oncol* 104:323–332. doi: 10.1002/jso.21943.

9. Shimizu S, Kamiike W, Hatanaka N, Yoshida Y, Tagawa K, Miyata M, et al. (1995). New method for measuring ICG Rmax with a clearance meter. *World J Surg* 19:113–118. doi: 10.1007/bf00316992.
10. Speich R, Saesseli B, Hoffmann U, Neftel KA, Reichen J (1988). Anaphylactoid reactions after indocyanine-green administration. *Ann Intern Med* 109:345–346. doi: 10.7326/0003-4819-109-4-345_2.
11. Obana A, Miki T, Hayashi K, Takeda M, Kawamura A, Mutoh T, et al. (1994). Survey of complications of indocyanine green angiography in Japan. *Am J Ophthalmol* 118:749–753. doi: 10.1016/s0002-9394(14)72554-1.
12. Tobis S, Knopf J, Silvers C, Yao J, Rashid H, Wu G, et al. (2011). Near infrared fluorescence imaging with robotic assisted laparoscopic partial nephrectomy: initial clinical experience for renal cortical tumors. *J Urol* 186:47–52. doi: 10.1016/j.juro.2011.02.2701.
13. Borofsky MS, Gill IS, Hemal AK, Marien TP, Jayaratna IS, Krane LS, et al. (2013). Near-infrared fluorescence imaging to facilitate super-selective arterial clamping during zero-ischaemia robotic partial nephrectomy. *BJU Int* 111:604–610. doi: 10.1111/j.1464-410X.2012.11490.x.
14. Watanabe M, Tsunoda A, Narita K, Kusano M, Miwa M (2009). Colonic tattooing using fluorescence imaging with light-emitting diode-activated indocyanine green: a feasibility study. *Surg Today* 39:214–218. doi: 10.1007/s00595-008-3849-9.
15. Hagen A, Grosenick D, Macdonald R, Rinneberg H, Burock S, Warnick P, et al. (2009). Late-fluorescence mammography assesses tumor capillary permeability and differentiates malignant from benign lesions. *Opt Express* 17:17016–17033. doi: 10.1364/OE.17.017016.
16. Jeschke S, Lusuardi L, Myatt A, Hruby S, Pirich C, Janetschek G (2012). Visualisation of the lymph node pathway in real time by laparoscopic radioisotope- and fluorescence-guided sentinel lymph node dissection in prostate cancer staging. *Urology* 80:1080–1086. doi: 10.1016/j.urology.2012.05.050.
17. Dindo D, Demartines N, Clavien PA (2004). Classification of surgical complications: a new proposal with evaluation in a cohort of 6336 patients and results of a survey. *Ann Surg* 240:205–213. doi: 10.1097/01.sla.0000133083.54934.ae.
18. Chauhan S, Coelho RF, Rocco B, Palmer KJ, Orvieto MA, Patel VR (2010). Techniques of nerve-sparing and potency outcomes following robot-assisted laparoscopic prostatectomy. *Int Braz J Urol* 36:259–272. doi: 10.1590/s1677-55382010000300002.
19. Kumar A, Samavedi S, Bates A, Coelho R, Rocco B, Marquinez J, et al. (2015). Using Indocyanine Green and Near-Infrared Fluorescence Technology to Identify the “Landmark Artery” During Robot-Assisted Radical Prostatectomy. *Videourology* 29:null. doi: 10.1089/vid.2014.0071.
20. Mangano MS, De Gobbi A, Beniamin F, Lamon C, Ciaccia M, Maccatrozzo L (2018). Robot-assisted nerve-sparing radical prostatectomy using near-infrared fluorescence technology and indocyanine green: initial experience. *Urologia* 85:29–31. doi: 10.5301/uj.5000244.
21. Salonia A, Castagna G, Capogrosso P, Castiglione F, Briganti A, Montorsi F (2015). Prevention and management of post prostatectomy erectile dysfunction. *Transl Androl Urol* 4:421–437. doi:

Tables

Table 1. Patient characteristics at baseline.

Clinical characteristics	Patients (n=91)
	Mean±standard deviation (median; Q1-Q3) ^a or n (%)
Age, years	67.8±5.9 (68; 64-72)
Prostate-specific antigen level (serum), ng/ml	6.7±1.8 (6.7; 5.3-7.8)
Body Mass Index, kg/m ²	29.6±5.5 (29; 25-33)
T stage	
T1	0
T2a	7 (7.7)
T2b	36 (39.6)
T2c	48 (52.8)
Gleason score	
6	53 (58.2)
7 ^a	21 (23.1)
8	13 (14.3)
9	3 (3.3)
10	1 (1.1)
SHIM score	16.7±3.5 (18; 15-19)
Erectile dysfunction severity	
Mild	61 (67.0)
Mild-moderate	24 (26.4)
Moderate	4 (4.4)
Severe	2 (2.2)

^a Respectively representing 50%; 25%-75% of the distribution; ^b 3+4 (one patient) or 4+3 (20 patients). SHIM, Sexual Health Inventory for Men.

Table 2. Sexual Health Inventory for Men (SHIM) score before and after surgery.

SHIM score	Patients (n=91) Mean±standard deviation (median; Q1-Q3) ^a	Change from baseline, mean	p-value *
Baseline	16.7±3.5 (18; 4-21)		
3 months	14.4±4.4 (16; 3-20)	-2.3	<0.001
6 months	15.2±4.4 (17; 3-21)	-1.6	0.008
9 months	16.2±4.0 (17; 3-21)	-0.5	0.331

^a Respectively representing 50%; 25%-75% of the distribution. * p-values <0.05 considered statistically significant (bold).

Table 3. Evolution in Sexual Health Inventory for Men score from baseline to 9 months after surgery.

	Patients (n=91), n (%)		
	Deterioration	Stable	Improvement
3 months	46 (50.5)	41 (45.1)	4 (4.4)
6 months	39 (42.9)	47 (51.6)	5 (5.5)
9 months	22 (24.2)	57 (62.6)	12 (13.2)

Deterioration, change <0; stable, change=0; Improvement, change >0.

Figures

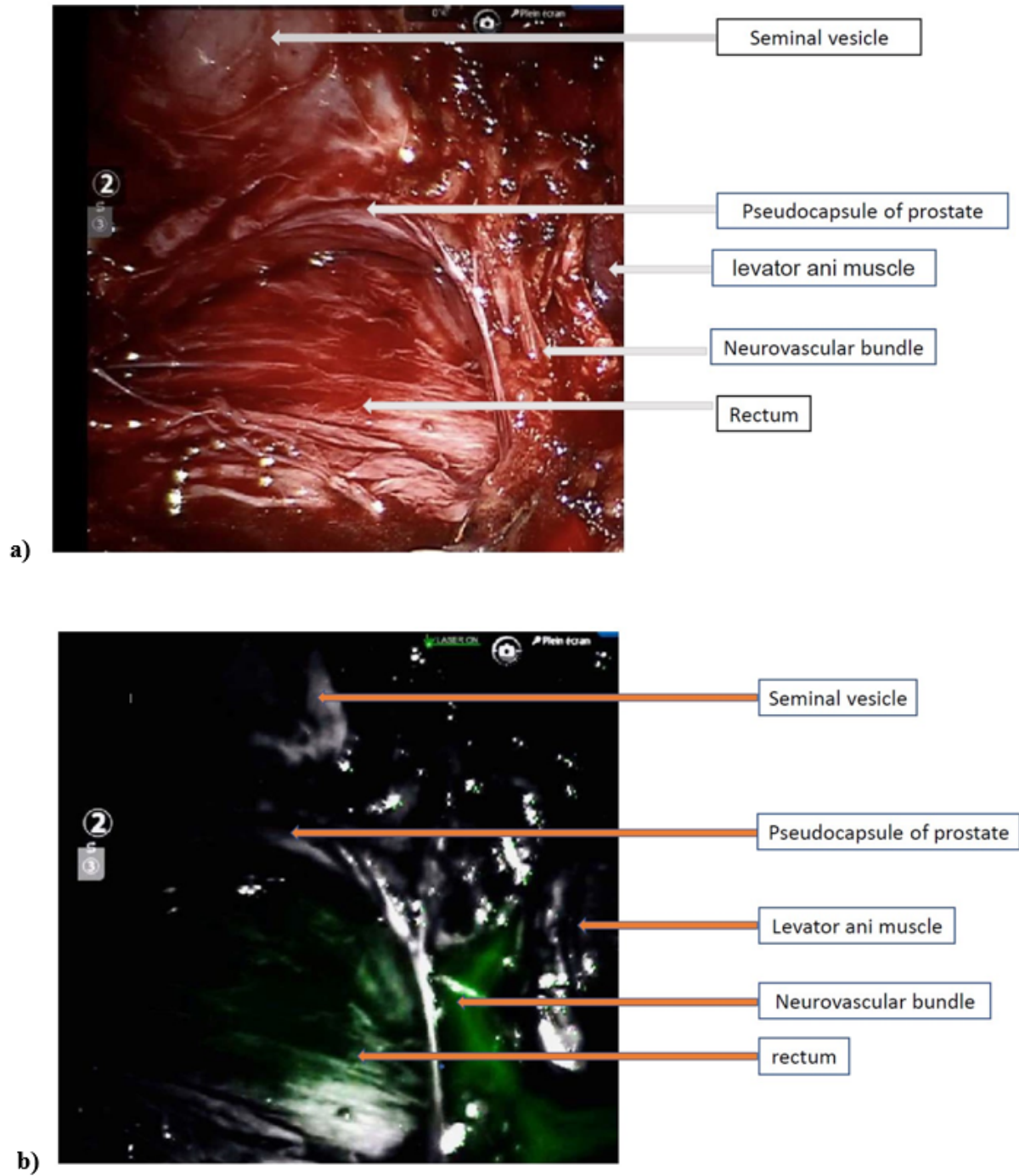


Figure 1

a) Standard light; b) near infrared fluorescence with indocyanine green.

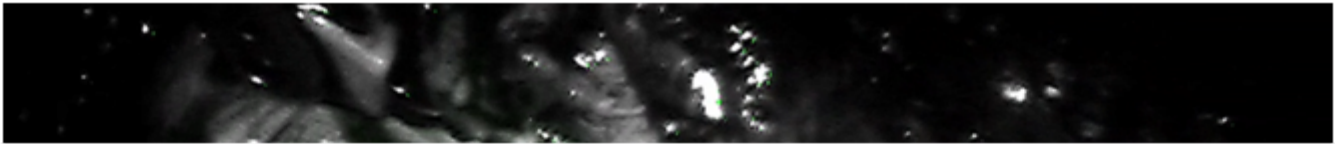


Figure 2

Microdissection of the neurovascular bundle is performed using non-electrified scissors and the Hem-o-lok Ligation System (Teleflex, USA).

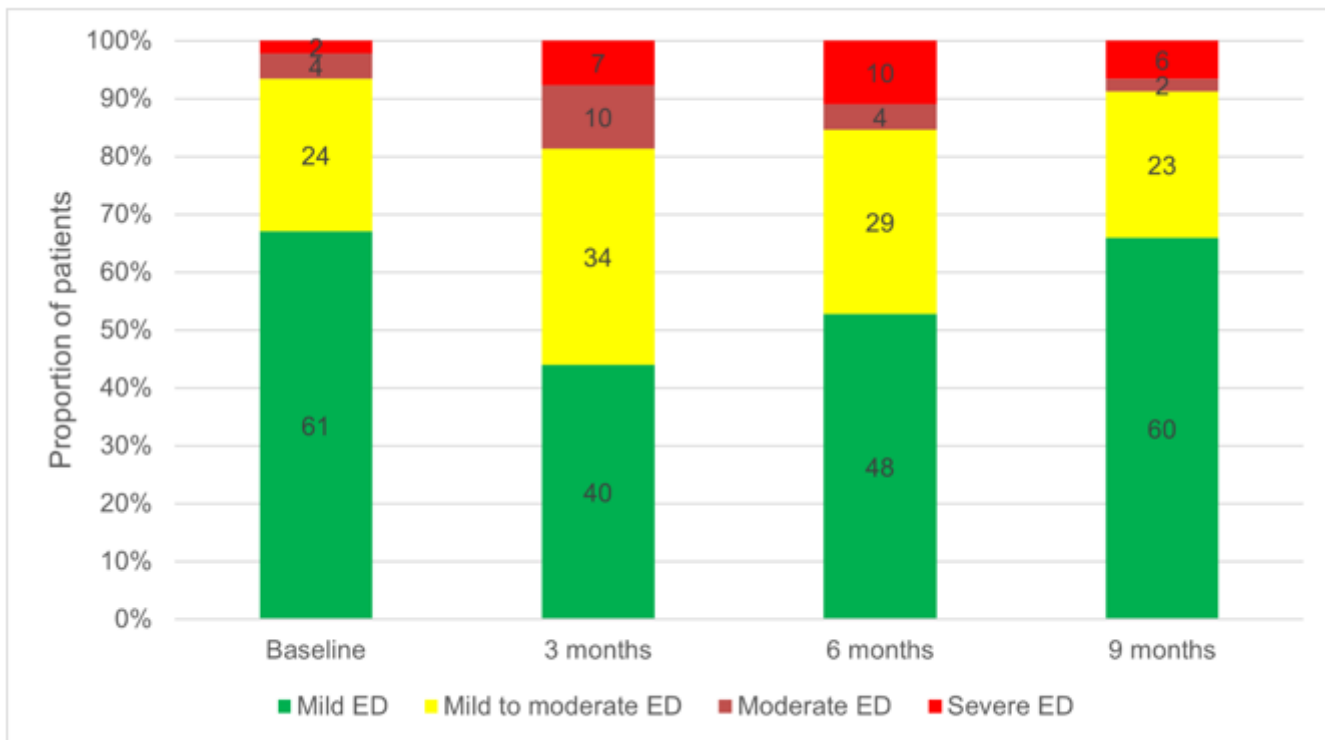


Figure 3

Evolution of erectile dysfunction (ED) categories (assessed using the SHIM) after surgery.

Supplementary Files

This is a list of supplementary files associated with this preprint. Click to download.

- [ICGinangiographicsurgerySupplementaryTable1.pdf](#)
- [ICGinangiographicsurgerySupplementaryvideo.mp4](#)